**Journal of Materials Science & Surface Engineering, 6(2): 773-778**
ISSN (Online): 2348-8956; 10.jmsse/2348-8956/6-2.3

# Parallel Evolution of Microstructure and Mechanical Properties of Bioglass/Hydroxyapatite Composites

**A.N. Fauzana[1] . K.A. Matori[2] . R.S. Azis[2] . N. Zainuddin[3] . B.N. Fadilah[1] . N.A. Zarifah[2] . M.H.M. Zaid[2]**

[1]Advanced Materials and Nanotechnology Laboratory, Institute of Advanced Technology, University Putra Malaysia, 43400 UPM Serdang, Selangor, Malaysia.
[2]Department of Physics, Faculty of Science, University Putra Malaysia, 43400 UPM Serdang, Selangor, Malaysia.
[3]Department of Chemistry, Faculty of Science, University Putra Malaysia, 43400 UPM Serdang, Selangor, Malaysia.

ABSTRACT
The purpose of this research work is to establish the parallel evolution stages of microstructure and mechanical properties development as well as their relationship. This kind of observation is not present in the literature of this research area and studies of the relationship between microstructure and mechanical properties have been directing towards the product of final sintering temperature, largely neglecting the parallel evolution of microstructure and mechanical properties and their relationship at various selected sintering temperature. Commercial bioglass (BG) of $SiO_2$–$CaCO_3$–$Na_2O_3$–$P_2O_5$–$CaF_2$ were prepared by conventional melt quenching technique and mixed with hydroxyapatite (HA) via solid state reaction. To complete the evolving series of temperature, the pellet samples were subjected to sinter from 500 to 1000°C with 50°C increments. Sintered sample were characterized by Differential Scanning Calorimetry (DSC), X-ray Diffractometry (XRD), Field Emission Scanning Electron Microscope (FESEM) and Archimedes Principle. Hardness and compressive strength was determined using Vickers Microhardness Tester and Universal Testing Machine (UTM) respectively. Results are implying that a high densification and mechanical regime is reached after sintering at low temperature (500 to 800°C) while low densification and mechanical regime is reached after sintering at higher temperature (850 to 1000°C). BG-HA sintered at 800°C presented the best results, with high relative density, hardness and compressive strength of 250 HV and 103 MPa, respectively.


ARTICLE HISTORY
Received 18-02-2018
Revised 22-02-2018
Accepted 09-03-2018
Published 02-04-2018

KEYWORDS
Bioglass,
Hydroxyapatite,
Microstructure,
Mechanical Properties

## Introduction

The development of new materials for the effective repair of the skeletal system is an important objective in biomaterial science [1]. Bioactive ceramics such as BG and HA are considered are the most promising biomaterials, owing their capability to form direct bonds with living bone after implantations in bone defects [2]. BG widely used in numerous ways as in replacement of hips, knees, tendons and ligaments due to the appropriate such us compatibility, chemical stability and high wear resistance. HA have been extensively studied for its potential in variety of medical applications as HA is found to be the most stable calcium phosphate under physiological conditions [3]. On this basis, BG-HA composites are currently attracting increasing interest as bone substitution. These materials should cover a broad functional requirement, which includes microstructural and mechanical properties. During the past decades, major advances have been made in developing bioceramic microstructures, in order to obtain implant material with better mechanical properties [4].

The improvement in microstructure properties in dense sintered materials is the main stream approaches to enhance the mechanical properties of BG-HA composites. This necessitates the optimization of the mechanical properties of BG-HA composites via a careful understanding of the microstructure-mechanical properties. In particular, it is crucial to control mechanical properties by a full knowledge of microstructural evolutions during thermal treatments.

Therefore, this research project focuses on the mechanical properties in bulk with the observation of its microstructure. It is interesting to study experimentally how mechanical properties behave in BG-HA composites and the evolution with the microstructure. Extensive research had been merely carried out on samples at final sintering temperature by neglecting the parallel evolution of microstructure and mechanical properties and their relationship at various lower sintering temperatures in many years. Consequently, systematic studies on microstructure-mechanical properties evolutions at lower sintering temperatures are still absent in this biocomposite materials. Due to disregards to this purpose subject, evolution of obtaining data scheme with the starting sintering temperature by 500 to 1000°C could be initiate to explore the fundamental behavior of BG-HA composite samples.

## Experimental

### Sample Preparation

Glass materials having the following composition ($45\%SiO_2$-$24.5\%Na_2CO_3$-$14.7\%CaCO_3$-$6\%P_2O_5$-$9\%CaF_2$) reagent grade chemicals, all in wt% was prepared by melting for 5h at 1400ºC in an aluminum crucible. The melt was then quenched in water and dry milled to a fine powder (<45µm). Quenching was fast enough to retain a completely amorphous material, as verified by X-Ray diffraction (XRD).BG powders with an average particle size below 45mm were mixed by 10wt% of HA powders, to

Corresponding Author: A.N. Fauzana, Tel: +0124622598
Email: fauzana22@yahoo.com
Contents lists available at http://www.jmsse.in/ & http://www.jmsse.org/

obtain BG-HA composite. Commercial HA with an average particle size below 45mm was used. All calculation (in wt%) were made according to the required recipe for BG + 10wt% of HA content. The mixture was prepared by dry milling the contents for about 24h.

All the above compositions were compacted into pellet forms. For this, each 1g of composite powder was uniaxial compacted in a cylindrical die of 10 mm in diameter and 3 mm in height at compacting pressure of 3 tonne. The pellets prepared were undergoesto sinter at eleven elevated sintering temperature ranging from 500 until 1000ºC with 50ºC increments for 3h sintering duration time.

Thermal characteristics of BG-HA composites were performed by Differential Scanning Calorimetry (DSC). Phase analysis for eleven sintered samples was performed by using X- Ray diffractometer using (PANalytical (Philips) X'Pert Pro PW3040/60) with CuKα radiation (λ = 1.54056Å). Microstructures of the sintered samples were examined using a Field Emission Scanning Electron Microscope (FESEM) using FEI NOVA NanoSEM 230. All the sintered samples were made conducting by sputter coating with gold. The density measurements were performed using the Archimedes principle and average grain size was measured by linear intercept method from the cross sectional surfaces of the FESEM images of BG-HA composite grain. Vickers microhardness were determined using Vickers Microhardness Tester with a load of 100kg. Meanwhile, compressive strength test was performed using Universal Testing Machine (UTM).

## Results and Discussion

### Thermal Analysis

Figure 1 shows the DSC curve. The DSC curves shows that the glass transition temperature, $T_g$ (endothermic effects) is observed at 550°C which has been reported extensively in the literature [5].The crystallization temperature, $T_{c1}$ (exothermic effects) is observed at 700°C meanwhile second crystallization temperature, $T_{c2}$ (exothermic effects) appears at 900°C.

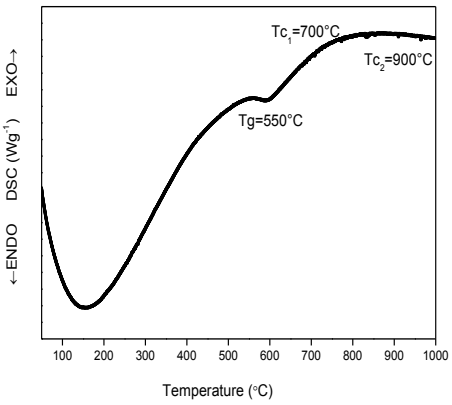


**Figure 1**: DSC curve for BG-HA composite

### Phase Analysis

The XRD pattern of BG-HA composite for as-prepared and powder sintered at various sintering temperature from 500 to 1000°C are shown in Figure 1. The XRD result for as-prepared powder takes amorphous states, indicative of internal disorder and it is worth mentioning that the powder didn't show any crystalline states. On the other hand, enhancement of crystallinity is achieved by treating the glass thermally at 500°C. XRD peaks become sharper and the amorphous hump nearly disappears after treating the glass at 500°C as clarified in Figure 1.The beginning of the separation of main intensity at 2θ = 32° into two peaks occurs at 600°C and intensifies at higher temperatures. [6] were revealed that the addition of $P_2O_5$ increased the extent of two phase separation and widens the range of phase-separable composition.The XRD patterns for sample sintered 600 and 650°C shows additional crystalline peaks, could be attributed to natrium calcium silicate ($Na_4CaSi_3O_9$), HA ($Ca_{10}(PO_4)_6(OH)_2$) and Fluoroapatite, FA ($Ca_5(PO_4)_3F$), in the range of 2θ = 50 to 70°. Furthermore, sample sintered at 700°C imply the presence of a new crystalline phase. The phase produced at 2θ = 35° are indicative of natrium calcium silicate ($Na_2Ca_3Si_6O_{16}$, JCPDS: 77-0410) which was formed at crystallization temperature ($T_c$) and retained its structure up to 800°C. Also, apparent broadening of the minor peak at 2θ = 29° occurs at 650 to 700°C, which attributed to $Na_4CaSi_3O_9$ respectively. It is obvious that the system of $SiO_2 - Na_2O - CaO - P_2O_5 - CaF_2$ has the tendency to form sodium calcium silicate crystalline phase of the $Na_2Ca_3Si_2O_8$ as the main crystalline phase.

The XRD patterns of sample sintered from 500 to 850°C show the presence of two phases of sodium calcium silicate of the formula ($Na_2Ca_3Si_2O_8$, JCPDS: 23-0670) and ($Na_4CaSi_3O_9$, JCPDS: 37-0282). Moreover, the formation of $Na_2Ca_3Si_2O_8$ and $Na_4CaSi_3O_9$ phases by thermal treatment, and also their enhanced intensity by temperature has been reported extensively by [7]. The minor peaks of apatite can also be seen in the range 2θ = 26 to 77° and indicated that both HA and FA are well crystallized. The presence of HA and FA peaks in accordance with JCPDS: 09-0432 and JCPDS: 34-0011 files respectively could be seen when sintering temperature from 500 to 800°C. As clearly observed, it is free of additional phases such as beta tricalcium phosphate (β-TCP) and CaO that indicates the thermal stability of samples [8]. Several peaks belonging to the HA and FA become more distinct and also the width of the peaks become more narrow, which suggested an increase in the degree of powder crystallinity as the sintering temperature increased from 500 to 800°C.

A transition is observed at 850°C, where there was no HA phase present, which means that HA were transformed to β-TCP ($Ca_3(PO_4)_2$). This is because at 850°C sintering temperature, HA became unstable and could potentially eliminate $OH^-$ to form decomposed of β-TCP [9]. By increasing the temperature from 900 to 1000°C, one can distinguish the presence of β-TCP and α-TCP. β-TCP and α-TCP was in agreement with JCPDS: 09-169 and 09-348 files respectively. The peaks belong to β-TCP and α-TCP retained as a minor phase at high sintering temperature (850 to 1000°C) as shown in Fig. 1. It can be seen that the decomposition of HA to β-TCP and α-TCP occurred in BG-HA composite as a result of poor thermal stability of HA at high sintering temperature [10]. An important reaction that has been reported at temperature above 850°C is the decomposition of HA to β-TCP.

$$Ca_{10}(PO_4)_6(OH)_2 \rightarrow 3\beta Ca_3(PO_4)_2 + CaO + H_2O \qquad (1)$$

It is also well established that β-TCP transforms to α-TCP at temperature of 1000°C

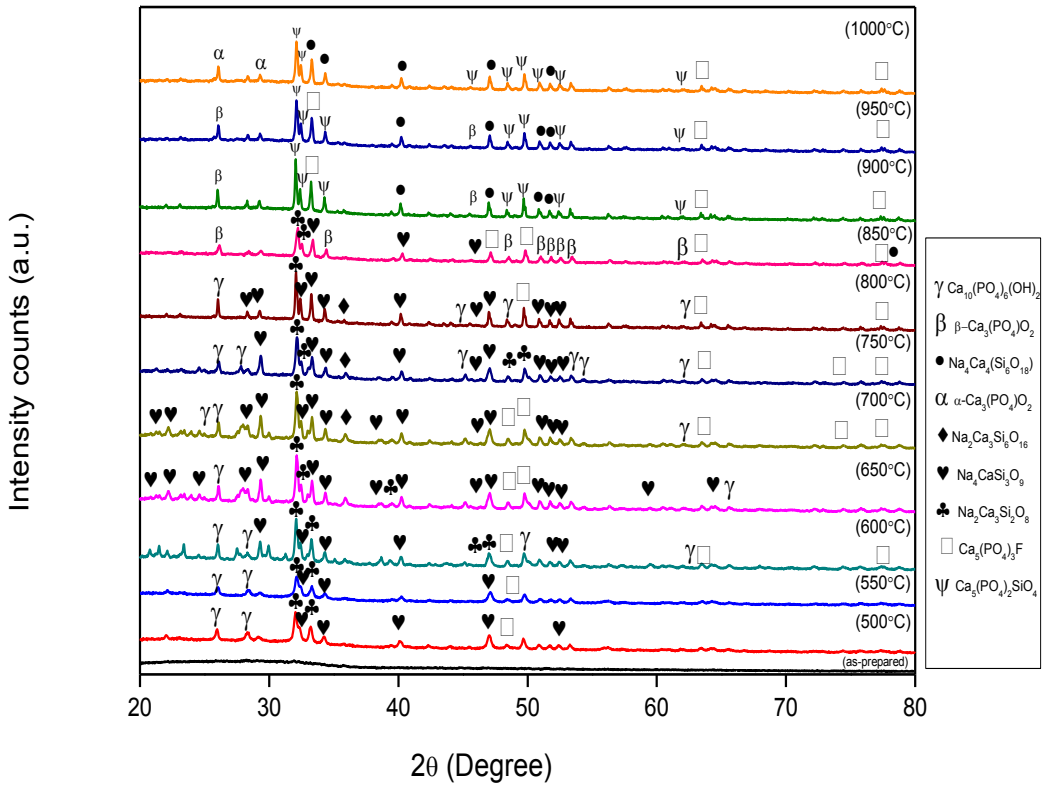


**Figure 2**: XRD patterns of pure BG-HA composite for as-prepared continued with sintering from 500 to 1000 °C

$$3\beta Ca_3(PO_4)_2 \rightarrow 3\alpha Ca_3(PO_4)_2 \quad (2)$$

The results agreed with the ones obtained in [11] works, that by sintering of BG and HA, a complete transformation of HA into α-TCP took place at 1000°C. This could be attributed to the presence of $Na_2O$ in the composite, giving rise to a high transformation of HA into α-TCP in BG-HA composites. Further increasing the temperature over 900 to 1000°C, the samples were composited by the well crystallized of combeite ($Na_4Ca_4(Si_6O_{18})$), FA, α-TCP, β-TCP and calcium phosphate silicate ($Ca_5(PO_4)_2SiO_4$). The XRD analysis at this temperature range showed that the main phase of this sample is apparently $Ca_5(PO_4)_2SiO_4$. The XRD patterns showed that FA retains its structure up to 1000°C. From Fig. 2, it can be noticed that the significant and sharp diffraction peaks of FA suggested that the high thermal stability of FA as compared to HA.

**Microstructure Observation, Densification and Grain Size**

The microstructure observations for the eleven pellets sintered from 500 to 1000°C were revealed from SEM micrographs as shown in Fig. 3 (a)-(k) respectively. The micrograph of the samples sintered at 500 to 650°C as shown in Fig. 3 (a)-(d) reveal the samples exhibits initial stage of sintering. This stages involved rearrangement of the powder particles in samples sintered at 500, 550 and 600°C, and formation of strong bonds or neck at the contact point between particles for samples sintered at 650°C. As shown in Fig. 3 (d), the dumbbell shape indicated that necking process occurred between the particles. Fig. 3(a)-(d) respectively exhibit porosity and become more severe for samples sintered at 650°C. This was attributed when necks were formed between particles in real powder compact, thus pores formed interconnected channels along grain edges. Additional observation from Fig. 3(b), indicating the glass transition temperature, $T_g$ occurred at 550°C. SEM micrograph of the samples sintered at 650°C shows slightly increase in grain size which was confirmed by grain size measurement. An increase in grain size was contributed by the coalescence phenomena during liquid phase sintering. Coalescence is a possible stage of densification, continued by a process of directional grain growth [12].

SEM micrograph of the samples sintered at 700°C as shown in Fig. 3 (e), shows the results of crystallization, which was confirmed by TGA-DSC analysis. The crystallization phenomena leading to viscosity increased and the sintering is actually stopped at 700°C [13]. This explanation is supported by Fig. 3 (e) that shows the crystallization at the surface of the particle with residual porosity, since the crystallization hinders the viscous flow, resulting detrimental to pore closure [14]. Obviously, increase in grain size and the presence of agglomeration can be observed at 750°C, identified in Fig. 3(f) which is difficult for the homogenization of the final microstructure of sintered samples. High agglomerations of BG-HA powder phenomenon caused the difficulty on the uniform spreading of the liquid phase during sintering, resulting highly porous network microstructure [15].

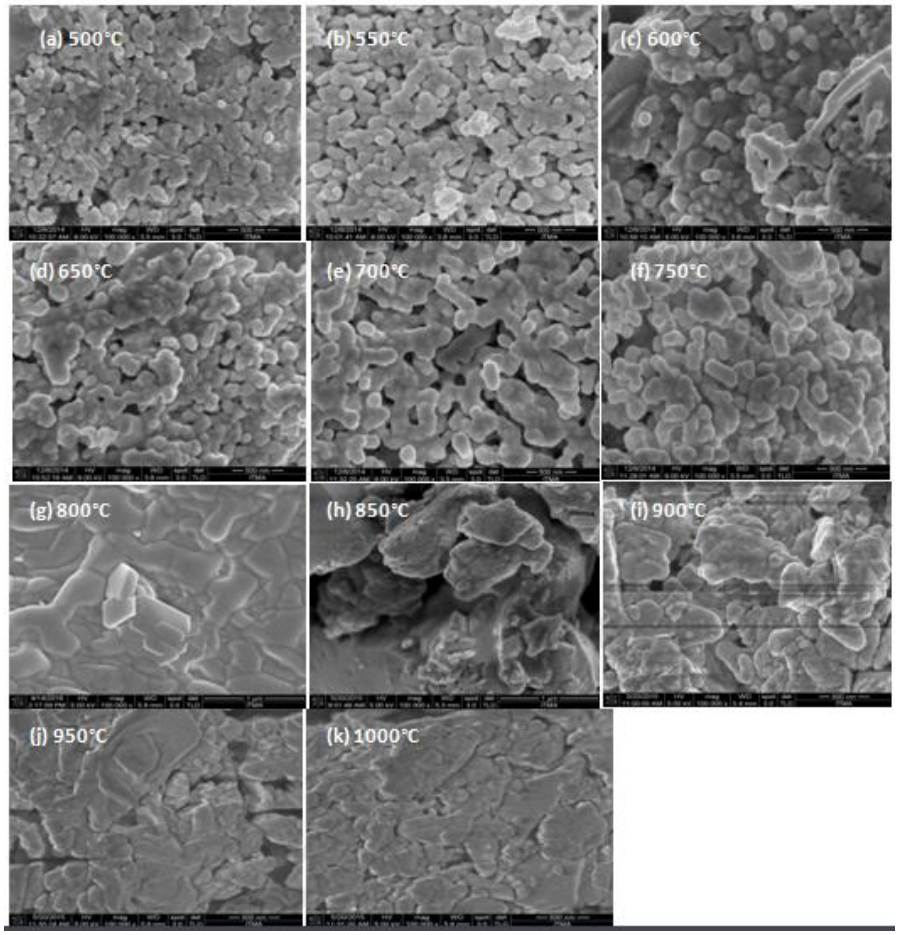


**Figure 3**: (a)-(k) FESEM micrograph of BG-HA composite sintered from 500 to 1000 °C

Large particles of faceted shape for the sample sintered at 800°C as shown in Fig. 3 (g) were observed. This result indicated that high degree of crystallization compared to sample sintered at lower temperature [16]. SEM micrograph of the samples sintered at 800°C and as shown in Fig. (g) exhibit completely changed in the microstructure. It is very important to note that the densification for both sintered sample was perceptibly improved which was contributed by less porosity with BG-HA particles homogenously distributed in the matrix. All the grain boundaries are closely packed with small amount of surface pore structure which was noticeable at the grain. This clearly shows that sintering process enhanced physical densification. It was clear shown that the porosity decreased obviously for the sample sintered at 800°C. As the sintering proceeds, the pore channels are disconnected and isolated pores were formed. Microstructural homogenization at both sintered samples was due to the viscous flow into the isolated pores by pore filling mechanism. Pore filling mechanism resulting the elimination of pores which requires grain growth and grain shape accommodation, by giving a high dense microstructure. High thermal stability of both sintered sample could be the best reason for less pore obtained at 800°C sintering temperature. The substitution of $F^-$ ions from $CaF_2$ into $OH^-$ ions, improved thermal stability of BG-HA composite which is retarded the decomposition process of HA, hence reducing the porosity.

SEM micrograph of the sample sintered at 850 to 1000°C as shown in Fig. 3 (h)-(k) shows abnormal grain growth with plate like structure. The microstructural transition of grain growth from normal to abnormal has been observed to occur with temperature change. As the sintering proceeds, abnormal grain growth occurs and as a result, more than one type of growth behavior may occur in the matrix systems [17]. In addition, sample sintered from 850 to 1000°C exhibit an intragranular pore. Intragranular pores are trapped pores in the grains due to the rapid grain growth. The pores trapped in the abnormal grain as shown in Fig. 3(h)-(k) are difficult to remove. The presence of both abnormal grain growth and intragranular pores are known to be bad inclusion which limits the attainment of high density, resulting the detrimental to the microstructure and mechanical properties of BG-HA composite.

Samples sintered at 850 to 1000°C are also characterized by a porous network, since in this way; it was possible to densify the samples at a relatively high temperature. As the increasing of high temperature, the sample did not provide sufficient mechanical stability due to the higher porosity. The existence of higher porosity as shown in Fig. 3(h)-(k) were attributed to the decomposition of HA. During decomposition process, $OH^-$ group was released from HA thus eliminate the hydrated water ($H_2O$) which leaves a vacancy from (pores) as can be referred by equation 1.This was further confirmed by XRD analysis by the presence of β-TCP, α-TCP and $Ca_5(PO_4)_2SiO_4$ phases which responsible for the formation of higher porosityat 850 to 1000°C. Further decomposition occur as the increasing of sintering temperature with large loss of $OH^-$ groups, thus more pore

were form which is reflected in the decrease in densification [18].

The evolution of densification and grain size with temperature are shown in Figure 3 and the value was listed in Table 1 respectively. The densification was perceptibly improved from 500 until 800°C sintering temperature and high regime of high densification was actually achieved at 850°C sintering temperature. However, the densities decrease obviously from 800 to 1000°C sintering temperature. From the images, it can be found that the grain size become larger as the sintering temperature increases. Slow rate of grain growth could be observed to occur at 500 to 700°C, continued by moderate increased at 750 and 800°C respectively. Lastly, the grain growth was observed to be aggressively increased at 850 up to 1000°C with the formation of abnormal grain growth.

**Table 1**: Density and grain size value for BG-HA composite.

| Sintering temperature (°C) | Density ($g/cm^3$) (±0.01) | Grain size (nm) (±0.1) |
|---|---|---|
| 500 | 1.615 | 60 |
| 550 | 1.511 | 70 |
| 600 | 1.577 | 150 |
| 650 | 2.032 | 180 |
| 700 | 2.83 | 220 |
| 750 | 2.87 | 250 |
| 800 | 2.95 | 320 |
| 850 | 1.55 | Abnormal |
| 900 | 1.52 | Abnormal |
| 950 | 1.47 | Abnormal |
| 1000 | 1.30 | Abnormal |

### Mechanical Properties

The evolution of hardness and compressive strength with temperature are shown in Fig. and 4 and 5 respectively. Graph plotted indicated that hardness and compressive strength was improved from 500 until 800°C sintering temperature. In conjunction with densification, improves mechanical strength is a result of fewer pores presented in the sample. Better densification values presented as the increasing of sintering temperature are related to the liquid phase comparatively; the increase of the sintering temperature reduce the liquid viscosity, increasing the particle attraction, resulting better spreading of the liquid around the grains, which facilitates the eliminating of pores and reduction of the undesirable accumulation of the glassy phase in triple junction, thus promotes high densification as well as hardness and compressive strength value [15]. Good wettening between the BG and HA phases and porosity eliminated resulted in increased density and mechanical strength. Furthermore, the viscous flow leads to a heterogeneous microstructure composed of large voids covered by crystalline phase and homogenous dense regions which had properly densified [14] hence improvement in hardness and compressive strength were obtained. High regime of hardness and compressive strength was actually achieved at 800°C sintering temperature with the value of 250HV and 103MPa respectively. It was also observed that the incorporation of $CaF_2$ in BG composition significantly improved the densification as well as mechanical properties of BG-HA composite. This resulted from the $F^-$ ion substitution into HA by decreasing the porosity. When a certain amount of $F^-$ ions substituted the $OH^-$ groups, a certain level of thermal stability was achieved. The $F^-$ ion concentration is sufficient to remove the crystal structure disorder of HA and hence stabilize the structure due to the alternating arrangement of the $F^-$ ions between each pairs of $OH^-$ groups [19]. High thermal stability effectively suppressed the HA decomposition, resulting reducing in porosity. As a result, dense bodies retaining with high densification and strength were obtained.

However, it was clearly shown that decrease in hardness and compressive strength obviously from 850 to 1000°C sintering temperature. This is due to the substantial decrease in density at high sintering temperature, as the materials reached high degree of porosity and formation of abnormal grain growth as was confirmed by FESEM observation. The porosity over the range of 850 to 1000°Cis related to the thermal decomposition products of HA, which reflected in the decrease in densification, hence become deleterious on mechanical strength. Clear decrease can be seen at 1000°C, indicating the decomposition and dehydroxylation process of HA leaves high amount of porosity, which limit the possibility of reaching high density as well as hardness and compressive strength [9]. This was consistent with [18] of pore formation associated with $OH^-$ release from HA during sintering, as can be referred by equation 1.

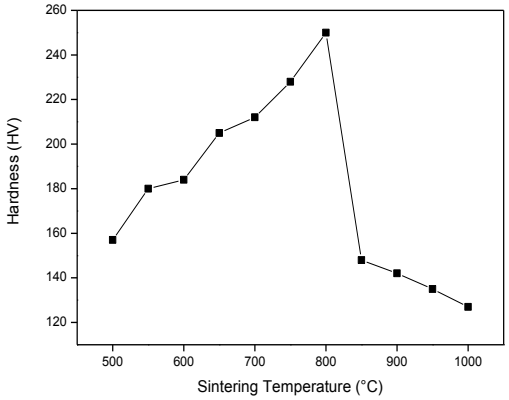


**Figure 4**: Variation of hardness for BG-HA composite sintered from 500-1000 °C

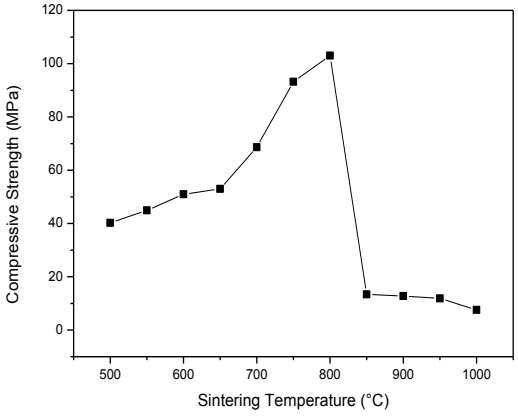


**Figure 5**: Variation of compressive strength for BG-HA composite sintered from 500-1000 °C

## Conclusions

The mechanical strength was improved significantly by sintering from 500-800°C. The optimal densification, hardness and compressive strength were achieved for

sample sintered at 800°C, reaching 2.95 g/cm$^3$, 250HV and 103MPa respectively. The improvement in mechanical properties was attributed to the improved densification. However, both hardness and compressive strength were decreased with further increasing sintering temperature from 850-1000°C. This study shows that the mechanical properties greatly depend on the microstructure properties at each stage of sintering temperature.

**Acknowledgement**
The authors are thankful to University Putra Malaysia (UPM) for providing Research University Grant Scheme (RUGS) and also to Ministry of Higher Education (MOHE) for providing the Fundamental Research Grant Scheme (FRGS) and MyBrain15 financial sponsorship.

## References

1. Bigi, A, Pazarolta, S, Roveri, N, Rubini, K, Bonelike Apatite Growth on Hydroxyapatite-Gelatin Sponges from Stimulated Body Fluid, Journal of Biomedical Materials Research Part A., 2001, 59(4), 709-715.
2. Liu, F.H, Synthesis of Bioceramics Scaffold for Bone Tissue Engineering by Rapid Prototyping Technique, Journal Sol-Gel Science Technology., 2012, 64, 704-710.
3. Sinha, A, Mishra, T, Ravishkandar, N, Polymer Assisted Hydroxyapatite Microspheres Suitable for Medical Applications, Journal Material Science Medical., 2008, 19, 2009-2013.
4. Tang, C.Y, Uskokovic, P. S, Tsui, C. D, Veljovic, D, Petrovic, R, Janakovic, D, Influence of Microstructure and Phase Composition on the Nanoindentation Characterization of Bioceramics Materials Based on Hydroxyapatite, Ceramics International., 2009, 35, 2171-2178.
5. Chatzistavrou, X, Zarba, T, Kontonasaki, E, Chrissafis, K, Koidis, P, Paraskeropoulos, K.M, Following Bioactive Glass Behaviour Beyond Melting Temperature by Thermal and Optical Methods, Physic State Solid., 2004, 201(5), 944-951.
6. Pallan, N.F, Matori, K.A, Lim, W.F, Quah, H.J, Fauzana, A.N, Rosnah, N, Khiri, M.Z.A, Farhana, S, Norhazlin, Z, Zarifah, N.A, Nurzilla, M, Hafiz, M.Z., Loy, C.W, Zamratul, M.I.M, Preparation of $SiO_2$-$Na_2O$-CaO-$P_2O_5$ Glass-Ceramic from Waste Materials and Heat Treatment Effects on its Morphology, Materials Science Forum., 2016, 846, 189-192.
7. Jurczyk, K, Niespodziana, K, Jurczyk, M.U, Jurczyk, M, Synthesis and Characterization of Titanium-4555 Bioglass Nanocomposites, Materials and Design, 2011, 32, 2554-2560.
8. Rameshbabu, N, Kumar, T.S.S, Rao, K.P, Synthesis of Nanocrystalline Fluorinated Hydroxyapatite by Microwave Processing and its In Vitro Dissolution Study, Bulletin of materials Science., 2006, 29, 611-615.
9. Oktar, F.N, Goller, G, Sintering Effects on Mechanical Properties of Glass Reinforced Hydroxyapatite Composites, Ceramics International, 2002, 28, 617-621.
10. Chen, Y, Miao, X, Thermal and Chemical Stability of Fluorohydroxyapatite Ceramics with Different Fluorine Contents, Biomaterials.,2005, 26(11), 1205-1210.
11. Santos, J.D, Knowles, J.C, Reis, R.L, Monteiro, Hastings, G.W, Microstructural Characterization of Glass-Reinforced Hydroxyapatite Composites, Biomaterials., 1994, 15(1), 5-10.
12. German, R.M, Suri, P, Park, S.J, Review: Liquid Phase Sintering, Journal Material Science, 2009, 44, 1-39.
13. Belucci, D, Sola, A, Cannillo, V. Bioactive Glass/$ZrO_2$ Composites for Orthopaedic Applications, Biomedical Materials, 2013, 9(1), 1-12.
14. Guillon, O, Cao, S, Boaccaccini, Effects of Uniaxial Lead on the Sintering Behaviour of 45S5 Bioglass Powder Compacts, Journal of the European Ceramic Society, 2011, 31(6), 999-1007.
15. Habibe, A.F., Maeda, L.D, Souza, R.C, Barboza, M.J.R, Daguano, J.K.M.F, Rogero, S.O, Santos, C, Effect of Bioglass Additions on the Sintering of Y-TZP Bioceramics, Materials Science and Engineering C, 2009, 29, 1959-1964.
16. Kim, S.K, Kim, Y.S, Bang, H.G, Park, S.Y, Synthesis of Bio-glass Ceramics in $Na_2 - CaO - SiO_2 - P_2O_5$ System with Fluoride Additives, Solid State Phenomena., 2007, 124-126, 759-762.
17. Kang, S.J.L, Lee, M.G. An, S.M, Microstructural Evolution during Sintering with Control of the Interface Structure, Journal American Ceramic Society, 2009, 92(7), 1464-1471.
18. Tancred, D.C, McCormark, Carr, A.J. A Quantitative Study of the Sintering and Mechanical Properties of Hydroxyapatite/Phosphate Glass Composites, Biomaterials, 1998, 19, 1735-1743.
19. Kutbay, I, Yilmaz, B, Evis, Z, Usta, M, Effect of calcium fluoride on mechanical behavior and sinterability of nano-hydroxyapatite and titania composites, Ceramics International., 2014, 40, 14817-14826.